Data Supplement for Potenza et al., Neural Correlates of Stress-Induced and Cue-Induced Craving: Influences of Sex and Cocaine Dependence, American Journal of Psychiatry (doi: 10.1176/appi.ajp.2011.11020289)

Supplementary Methods, Figures, and Tables

Methods

Participants

Individuals on medications for medical or psychiatric concerns were excluded, as were individuals needing detoxification for alcohol use. Subjects underwent a complete medical examination including electrocardiogram and laboratory tests as described previously (1). There were no exclusionary criteria for tobacco use. Cocaine-dependent subjects who were tobacco smokers typically continued smoking 1-2 cigarettes each during four scheduled smoke breaks throughout the day during their hospitalization stays. All cocaine-dependent subjects were abstinent from other drugs for several weeks prior to fMRI scanning (see Table 1 for mean length of abstinence).

An important aspect of the current study is the inclusion of social-drinking comparison participants who report alcohol-cue-induced craving and arousal but minimal stress-induced craving (2). As social drinkers have these characteristics in the absence of a psychiatric condition characterized by dysfunctional drug-seeking and using, they represent a particularly relevant comparison group to assess the effects of psychoactive substance use and abuse on stress and motivation circuits. Comparison subjects were determined to be medically healthy. Imaging sessions in women in both groups were tested during the follicular (days 4-11) or the luteal phases (days 15-25) as determined by self-report diaries and serum samples of estrogen and progesterone. Comparison men and women had not consumed alcohol for at least 72 hours prior to scanning.

Imagery Script Development

An important aspect is the use of both stress and substance cue conditions, both of which have been shown to induce craving and with potentially different clinical implications (1). Specific details regarding physical, interpersonal, cognitive, and bodily responses were obtained for the development of the scripts. Examples of stress situations included familial conflicts or work-related stress. Drug/alcohol-related situations involved descriptions of anticipation and consummatory phases of substance use (e.g., being at a bar and being offered cocaine, using cocaine with a drug-using buddy, etc.). Examples of neutral-relaxing situations included resting on the beach or a fall day in the park (detailed description of procedures are provided in (3).

Scripts of two minutes length each were developed and recorded on audiotape in the week prior to imaging. To reduce variability in imagery ability and train all subjects in progressive relaxation, a one-session relaxation and guided-imagery training session was conducted with all participants as conducted in previous studies of cocaine-dependent and comparison subjects (4, 5). This approach was used to help mitigate against influences of one fMRI run carrying over to the next. To reduce variability, one female investigator without discernable ethnicity read the scripts during audiotaping.

fMRI Acquisition

Individuals who were tobacco smokers were allowed to smoke approximately 45 minutes prior to fMRI scanning to avoid nicotine intoxication or withdrawal, as we have done previously (4). Subjects were positioned in the coil and head movements were restrained using foam pillows. Anatomical images of the functional slice locations were next obtained with spin-echo

imaging in the axial plane parallel to the anterior-commissure/posterior-commissure line with TR=300 msec, TE=2.5 msec, bandwidth=300 Hz/pixel, flip angle=60 degrees, field of view=220x220 mm, matrix=256x256, 32 slices with slice thickness=4mm and no gap. Functional, blood oxygen level dependent (BOLD) signals were then acquired with a single-shot gradient echo-planar imaging (EPI) sequence. Thirty-two axial slices parallel to the anterior-commissure/posterior-commissure line covering the whole brain were acquired with TR=2,000 msec, TE=25 msec, bandwidth=2004 Hz/pixel, flip angle=85°, field of view=220x220 mm, matrix=64x64, 32 slices with slice thickness=4mm and no gap, 190 measurements. At the end of the functional imaging, a high-resolution three-dimensional Magnetization Prepared Rapid Gradient Echo (MPRAGE) sequence (TR=2530 ms; echo time (TE)=3.34 ms; bandwidth=180 Hz/pixel; flip angle (FA)=7°; slice thickness=1mm; field of view=256 x 256mm; matrix=256 x 256) was used to acquire sagittal images for multi-subject registration.

fMRI Trials

Six fMRI trials (two each per condition) were acquired in a randomized, interdigitated, and balanced fashion. Each trial included a 1.5-min quiet baseline period followed by a 2.5-min imagery period (that included 2 min of read-imagery and 0.5 min of quiet-imagery) and a 1.5-min quiet recovery period. Before and after each scanning trial, subjects were asked to rate "how tense, jittery and anxious" they were feeling presently on a 0-10 scale. Subjects also rated their craving pre- and post-trial and the imagery vividness on 0-10 scales. Heart rate was monitored during scanning. Between imaging trials, subjects participated in progressive relaxation for 2 min periods to reduce any remaining anxiety or distress from prior trials. Time between trials (including the 2 min progressive relaxation period and the time to assess subjective responses)

was approximately three to four minutes. Subsequent fMRI trials were initiated after subjects' anxiety and heart rate measures had returned to their previous pre-trial baseline.

fMRI Analysis

All data were converted from Digital Imaging and Communication in Medicine (DICOM) format to analyze format using XMedCon (6). During the conversion process, the first 10 images at the beginning of each of the 6 functional series werediscarded to enable the signal to achieve steady-state equilibriumbetween radio frequency pulsing and relaxation, leaving 180 measurements for analysis. Images were motion corrected for three translational and three rotational directions (7). Trials with linear motion in excess of 1.5 mm or rotation greater than 2 degrees were discarded. Individual subject data were analyzed using a General Linear Model (GLM) on each voxel in the entire brain volume witha regressor (time during imagery) for each trial per condition relative to the baseline. The resulting functional images for each script type were spatially smoothed with an 8-mm Gaussian kernel to account for variations in the location of activation across subjects. The output maps were normalized beta-maps, which were in the acquired space (3.44mm x 3.44mm x 4mm). To take these data into a common reference space, three registrations were calculated with the Yale BioImage Suite software package (http://www.bioimagesuite.org/) (8). The first registration performs a linear registration between the individual subject raw functional image and that subject's two-dimensional anatomical image. The two-dimensional anatomical image is then linearly registered to the individual's three-dimensional anatomical image. The three-dimensional differs from the two-dimensional in that it has a 1x1x1 mm resolution whereas the two-dimensional z-dimension is set by slice-thickness and its x-y dimensions are set by voxel size. Finally, a non-linear registration is

computed between the individual three-dimensional anatomical image and a reference three-dimensional image. The reference brain used was the Colin27 Brain (9) which is in Montreal Neurological Institute (MNI) space (10) and is commonly applied in SPM and other software packages. All three registrations were applied sequentially to the individual normalized beta-maps to bring all data into the common reference space.

We generated a two-by-two-by-three random effects ANOVA in which sex (male, female), diagnostic group (cocaine-dependent, comparison) and condition (stress, drug/alcohol cue, and neutral-relaxing) were treated as fixed-effect factors and subject as a random-effect factor using the GroupAna program from the AFNI Matlab library (http://afni.nimh.nih.gov/afni/matlab/). Results were converted into ANALYZE format for viewing in BioImage Suite, using BioImage Suite's algorithms to transform data from MNI to Talairach space (11). A Family-Wise-Error rate correction for multiple comparisons was applied using Monte-Carlo simulations (12) conducted withAlphaSim in AFNI (13) and set at $p<.05$ for the overall factorial analysis (main effects and interactions and simple effects analysis).

Supplementary figures and tables follow below.

References

1. Sinha R, Garcia M, Paliwal P, Kreek MJ, Rounsaville BJ. Stress-induced cocaine craving and hypothalamic-pituitary-adrenal responses are predictive of cocaine relapse outcomes. Archives of General Psychiatry. 2006;63(3):324-31.
2. Fox HC, Hong KI, Siedlarz K, Sinha R. Enhanced sensitivity to stress and drug/alcohol craving in abstinent cocaine-dependent individuals compared to social drinkers. Neuropsychopharmacology. 2008 Mar;33(4):796-805.
3. Sinha R. Modeling stress and drug craving in the laboratory: Implications for addiction treatment development. Addiction Biology. 2009;14(1):84-98.
4. Sinha R, Lacadie C, Skudlarski P, Fulbright RK, Rounsaville BJ, Kosten TR, et al. Neural activity associated with stress-induced cocaine craving: A functional magnetic imaging study. Psychopharmacol. 2005;183:171-80.

5. Li C, Kosten TR, Sinha R. Sex Differences in Brain Activation During Stress Imagery in Abstinent Cocaine Users: A Functional Magnetic Resonance Imaging Study. Biol Psychiatry. 2005;57:487-94.
6. Nolfe E. XMedCon- An open-source medical image conversion toolkit. Eur J Nucl Med. 2003;30 (Supp.2):S246, TP39.
7. Friston KJ, Williams S, Howard R, Frackowiak RS, Turner R. Movement-related effects in fMRI time-series. Magn Res Med. 1996;35:346-55.
8. Duncan JS, Papademetris X, Yang J, Jackowski M, Zeng X, Staib LH. Geometric strategies for neuroanatomic analysis from MRI.Neuroimage. 2004;23Suppl 1:S34-45.
9. Holmes CJ, Hoge R, Collins L, Woods R, Toga AW, Evans AC. Enhancement of MR images using registration for signal averaging. J Comput Assist Tomogr. 1998 Mar-Apr;22(2):324-33.
10. Evans AC, Collins DL, Mills SR, Brown ED, Kelly RL, Peters TM, editors. 3D statistical neuroanatomical models from 305 MRI volumes.Nuclear Science Symposium and Medical Imaging Conference; 1993 31 Oct.-6 Nov.
11. Lacadie CM, Fulbright RK, Rajeevan N, Constable RT, Papademetris X. More accurate Talairach coordinates for neuroimaging using non-linear registration. Neuroimage. 2008;42.
12. Xiong J, Gao J-H, Lancaster JL, Fox PT. Clustered pixels analysis for functional MRI activation studies of the human brain. Human Brain Mapp. 1995;3:287-301.
13. Cox RW. AFNI: software for analysis and visualization of functional magnetic resonance neuroimages. Comput Biomed Res. 1996 Jun;29(3):162-73.

Figure S1. Condition-by-group interactions on changes in anxiety, craving, and heart rate. Self-reported changes in anxiety (a) and craving (b), and in heart rate (c) are shown for cocaine-dependent (dark bars) and comparison (light bars) subjects, averaged for the stress (S), drug cue (D) and the neutral (N) trials. Asterisks indicate contrasts between groups significant at $p<0.001$.

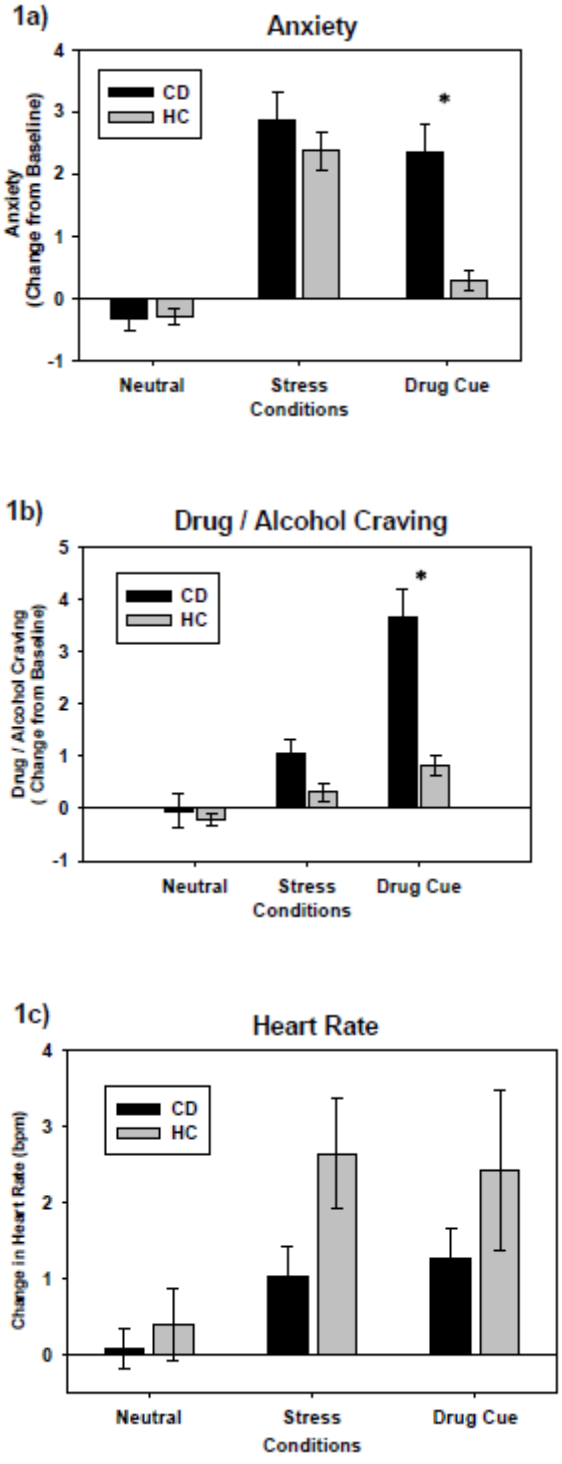

1d)

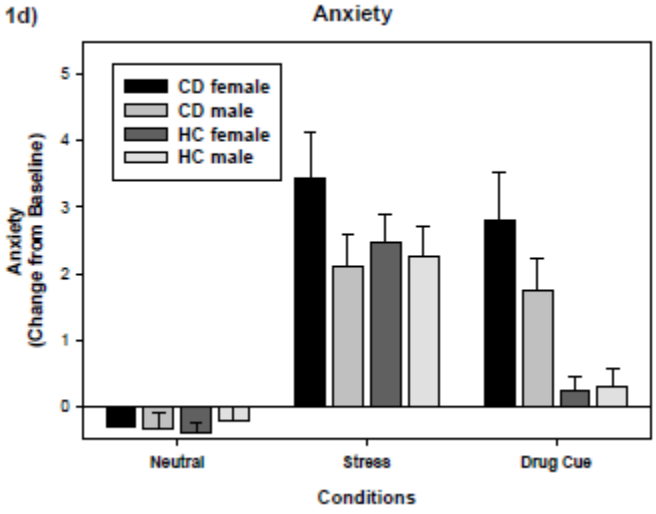
Anxiety
CD female
CD male
HC female
HC male
Anxiety (Change from Baseline)
0
1
2
3
4
5
Neutral
Stress
Drug Cue
Conditions

1e)

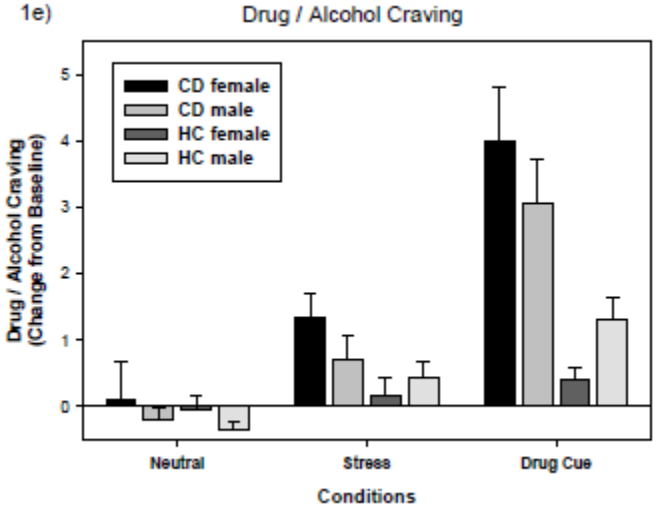
Drug / Alcohol Craving
CD female
CD male
HC female
HC male
Drug / Alcohol Craving (Change from Baseline)
0
1
2
3
4
5
Neutral
Stress
Drug Cue
Conditions

1f)

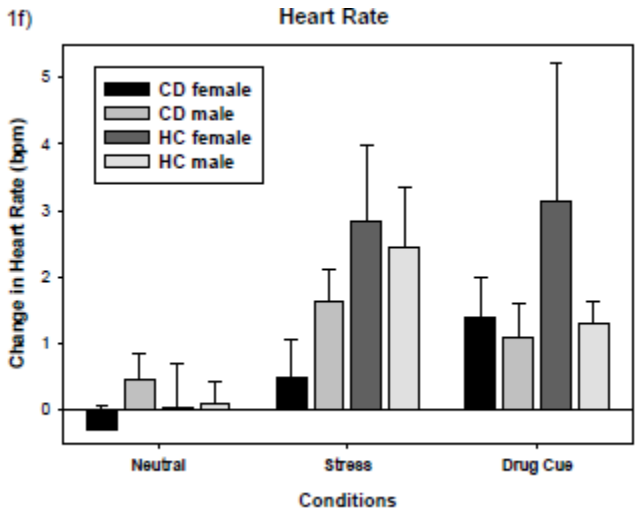
Heart Rate
CD female
CD male
HC female
HC male
Change in Heart Rate (bpm)
0
1
2
3
4
5
Neutral
Stress
Drug Cue
Conditions

Figure S2. Gender-by-diagnostic-group-by-condition interaction maps. Shown are axial brain sections highlighting regions showing significant 3-way interactions involving two gender groups (female, male), two diagnostic groups (cocaine-dependent, comparison) and three cue conditions (stress, substance and neutral-relaxing). The maps are thresholded at $p<0.05$, with a family-wise-error correction. Maps span from Talaraich z=-14mm (upper left) to z=49mm (lower right), at increments of 3-4 mm. The color bar indicates the strengths of interactions.

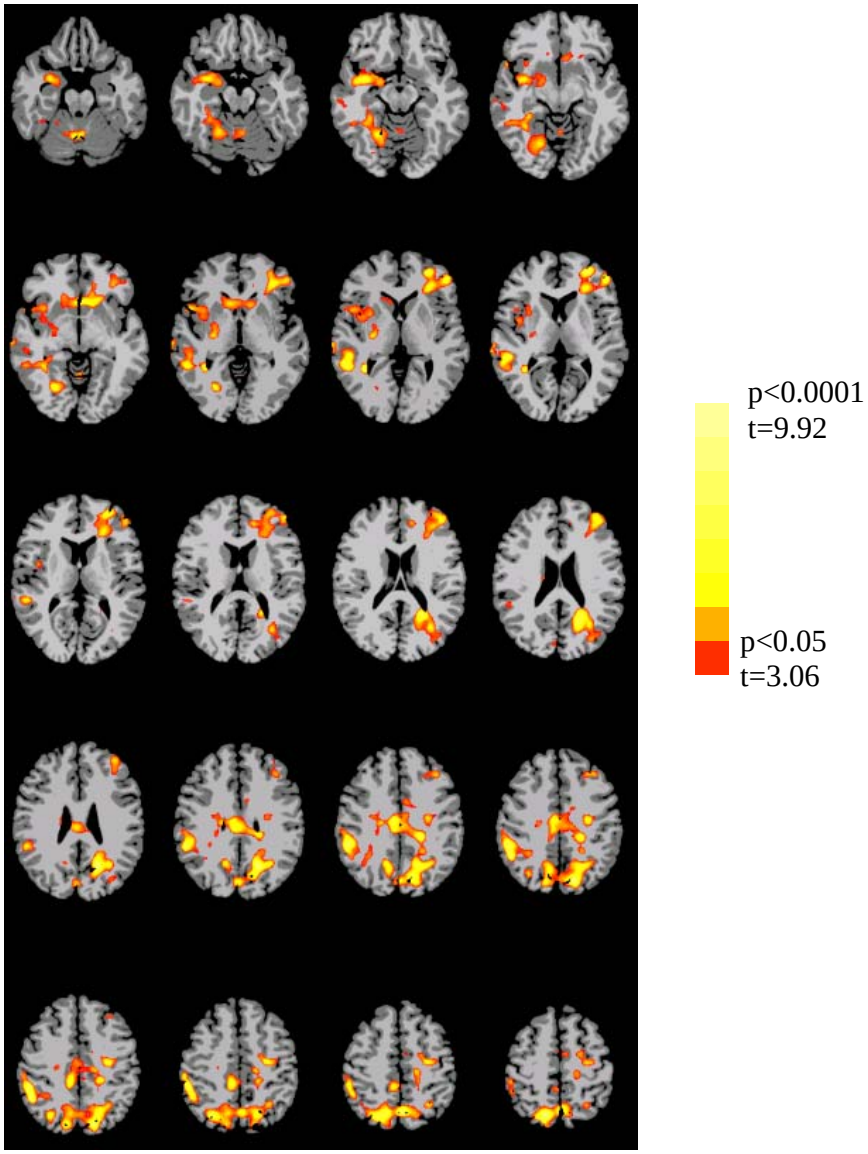

Figure S3. Brain activation maps highlighting main effects of condition. Brain maps highlighting main effects of condition in women (A) and men (B) are shown. Maps are thresholded at p<0.05, with a family-wise-error correction. Maps span from Talaraich z=-14 mm (upper left) to z=49 mm (lower right), at increments of 3-4 mm. Color bars indicate the strengths of interactions (A, B) or magnitudes of between-group differences (C, D, E).

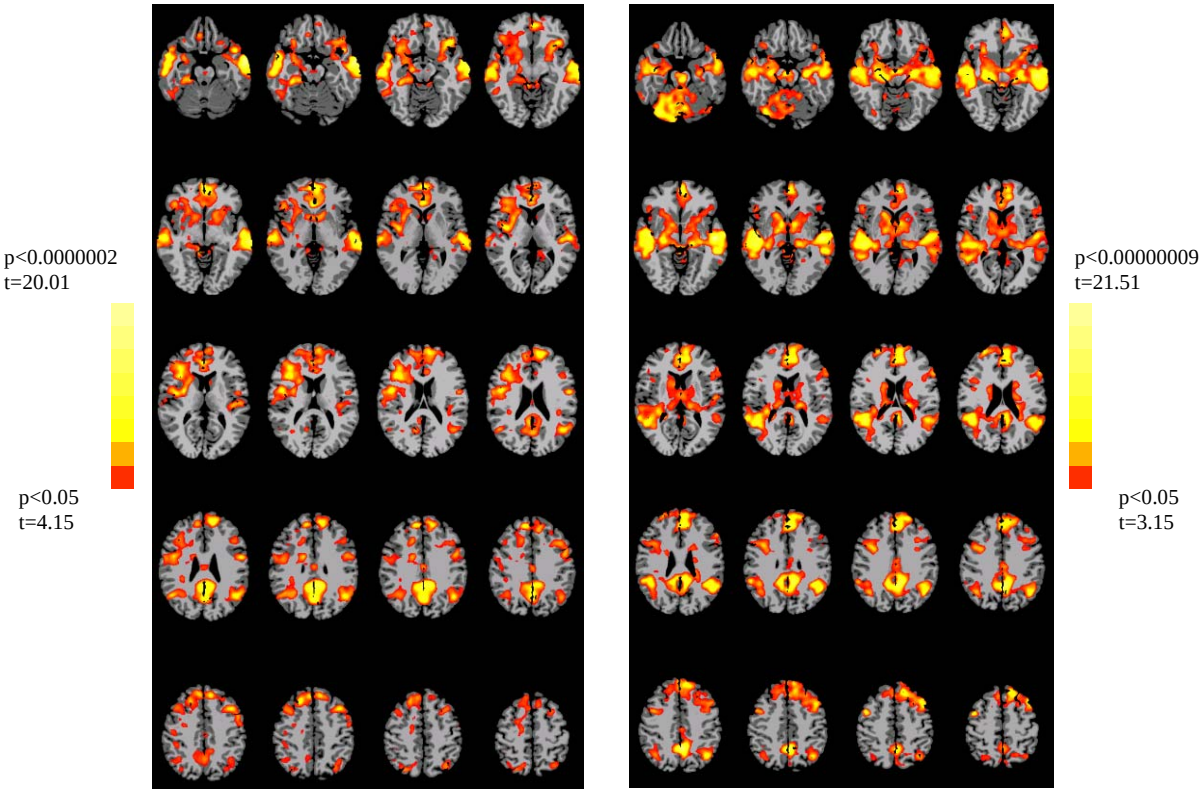

A) Women B) Men

Figure S4. Brain activation maps in women and men highlighting main effects of diagnostic group and group-by-condition interactions. Maps highlighting for women main effects of diagnostic group (cocaine-dependent, comparison) across conditions (A) and diagnostic-group-by-condition interactions (B) are shown. Maps highlighting for men main effects of diagnostic group (cocaine-dependent, comparison) across conditions (C) and diagnostic-group-by-condition interactions (D) are shown. Maps are thresholded at $p<0.05$, with a family-wise-error correction. Maps span from Talaraich z=-14mm (upper left) to z=49mm (lower right), at increments of 3-4 mm. Color bars indicate the strengths of interactions.

Panels A and B: Main and interactive effects in women

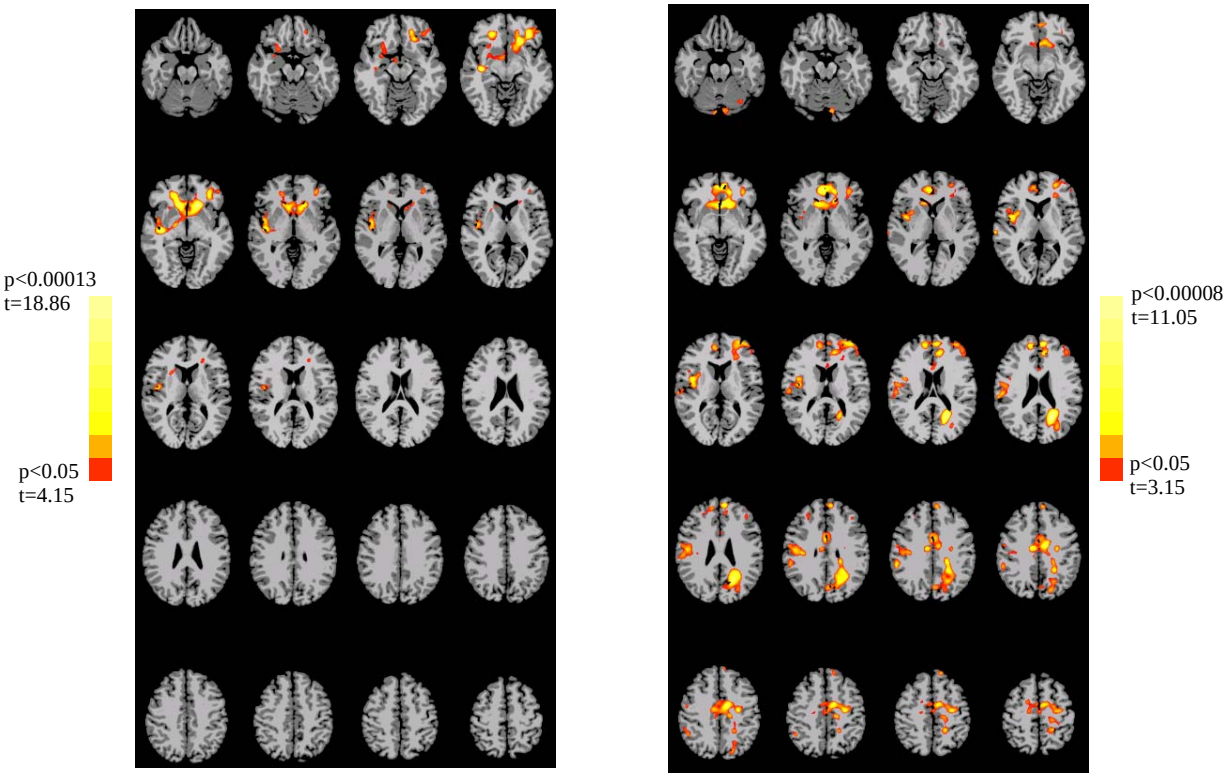

A) Main Effect Group B) Group-by-Condition Interaction

Panels C and D: Main and interactive effects in men

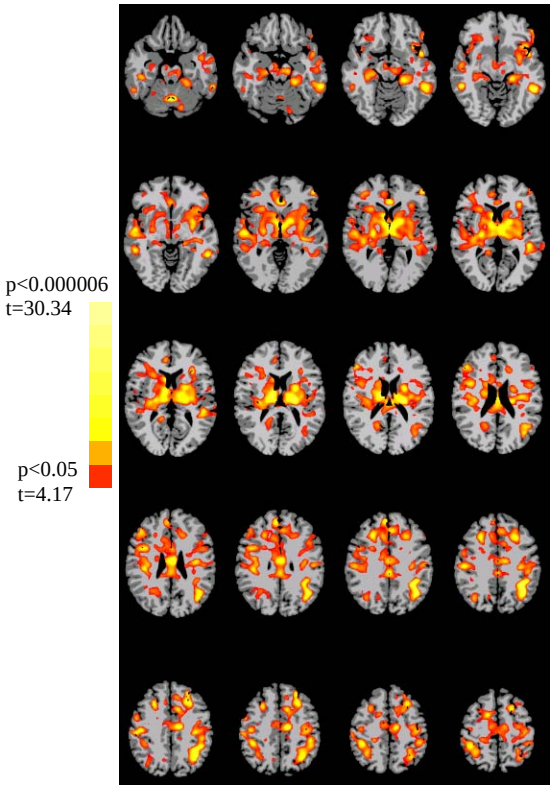

C) Main Effect Group

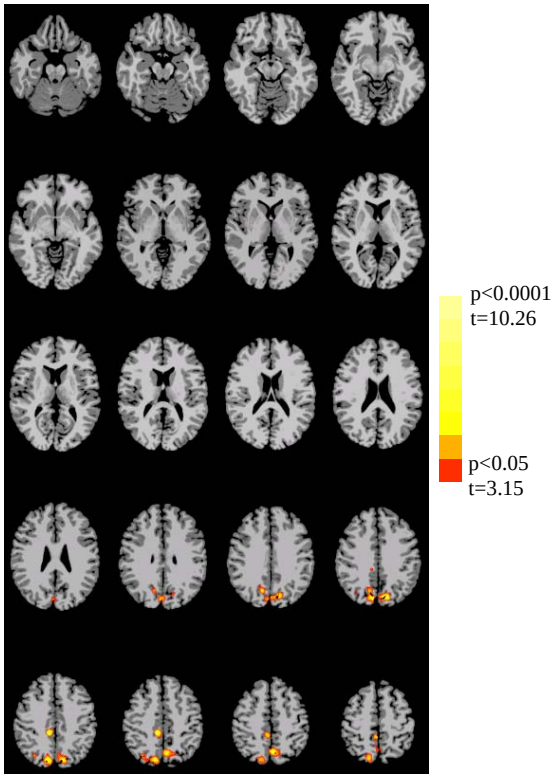

D) Group-by-Condition Interaction

Figure S5. Brain activation maps for women and men. Displayed are between-diagnostic-group contrast maps highlighting in yellow-red color regions where cocaine-dependent subjects show more activation than comparison ones and in blue-purple color regions where cocaine-dependent subjects show less activation than comparison ones during the stress (A, D), drug (B, E) and neutral-relaxing (C, F) conditions for women (A-C) and men (D-F). Maps are thresholded at $p<0.05$, with a family-wise-error correction. Maps span from Talaraich z=-14mm (upper left) to z=49mm (lower right), at increments of 3-4 mm. Color bars indicate the magnitudes of between-group differences.

Panels A, B, and C: Group differences in women:

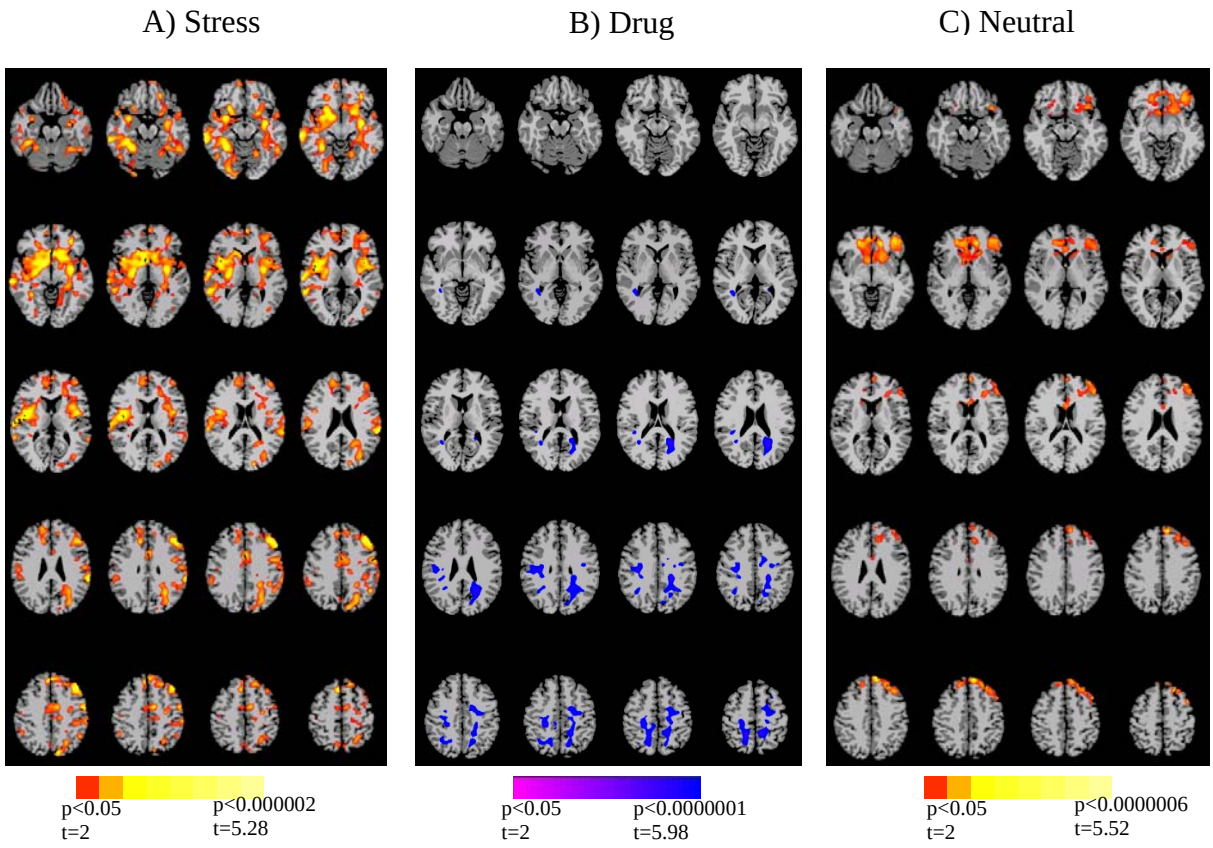

Panels D, E, and F: Group differences in men

D) Stress

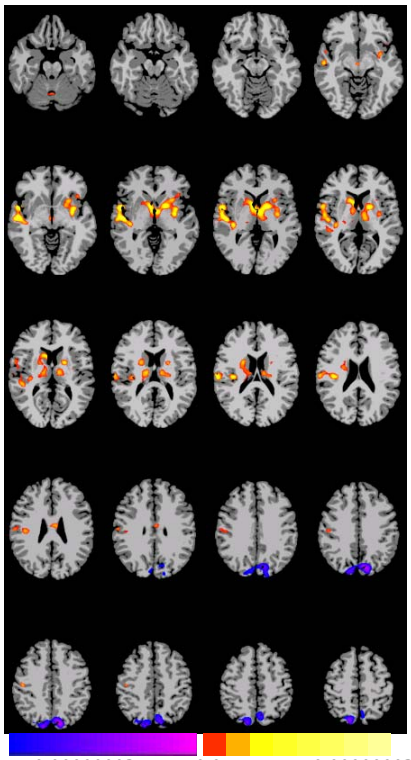

p<0.00000003 p<0.05 p<0.00000003
t=6.37 t=2 t=6.37

E) Drug

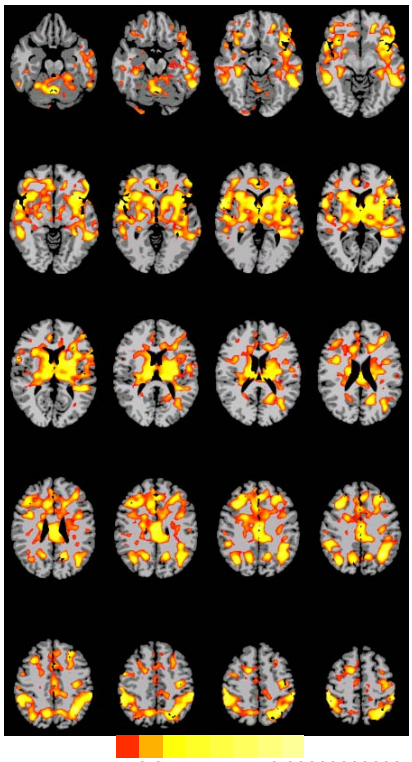

p<0.05 p<0.000000000004
t=2 t=8.64

F) Neutral

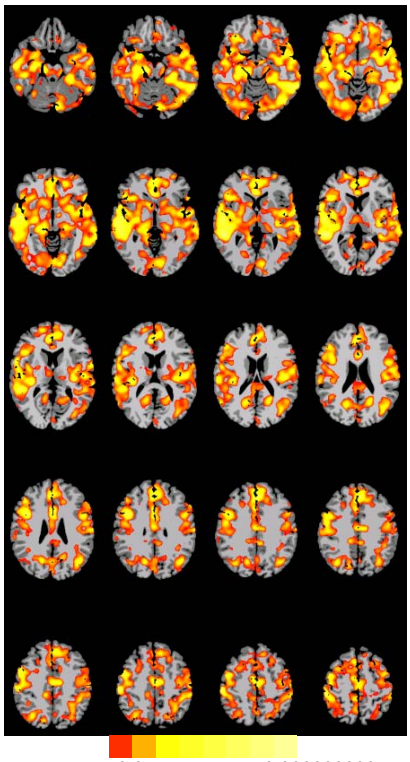

p<0.05 p<0.0000000001
t=2 t=7.73

Figure S6. Correlations between subjective craving scores and drug-cue- and stress-cue-related neural responses. Correlation maps in women are shown for subjective drug-cue-induced craving and neural responses to the drug cue condition (A). Correlation maps in men are shown for subjective drug-cue-induced craving and neural responses to the drug cue condition (B) and for subjective stress-cue-induced craving and neural responses to the stress cue condition (C). In all cases, the responses to the neutral cue condition are used as a comparison condition with the active condition in the correlational analyses. Maps are thresholded at $p<0.05$, with a family-wise-error correction. No correlation in women survived family-wise-error correction for stress-cue-induced craving and neural responses to the stress cue condition. Maps span from Talaraich z=-14 mm (upper left) to z=49 mm (lower right), at increments of 3-4 mm. Color bars indicate the strengths of correlations.

Panel A: Correlations in women

A) Drug-induced craving

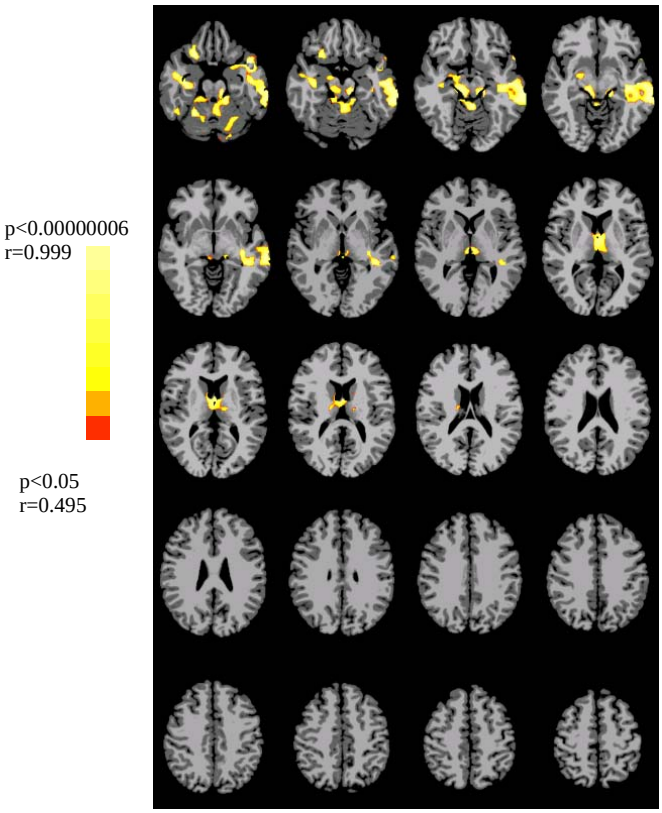

Panels B and C: Correlations in men

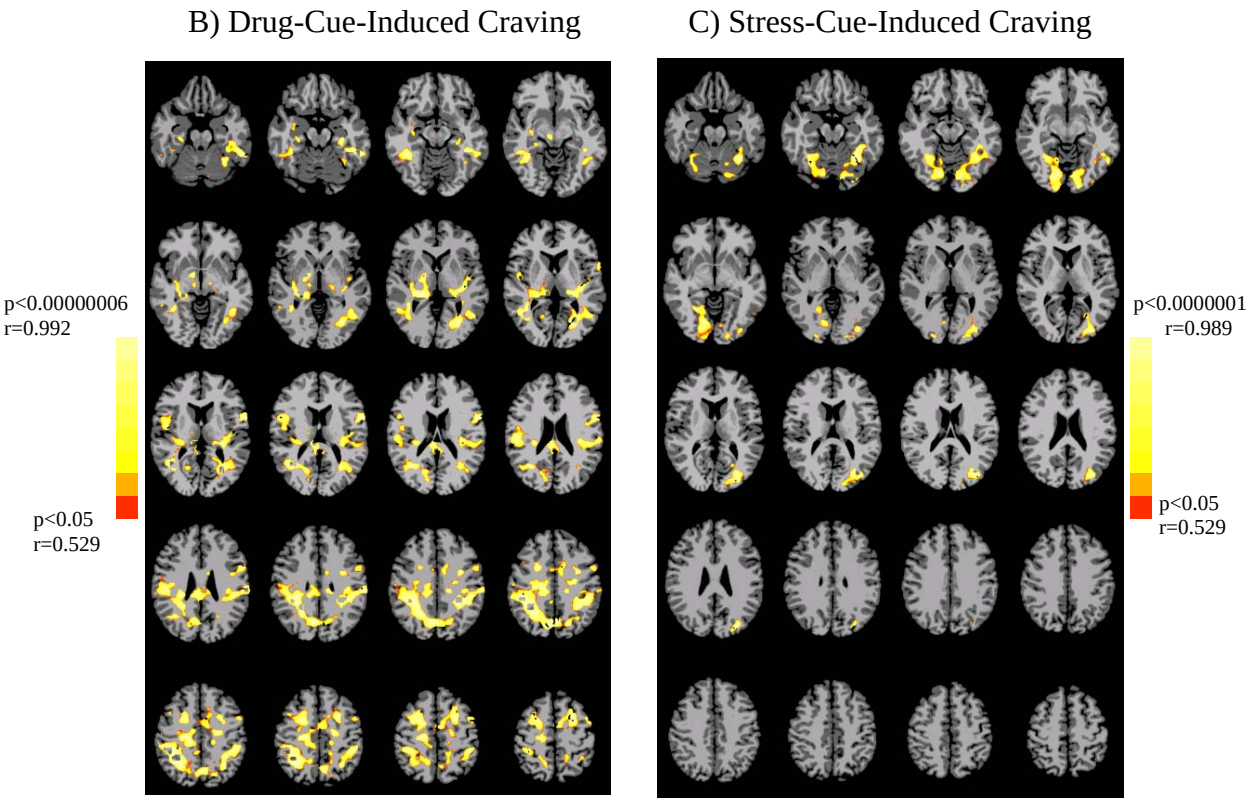

Table S1. Results of Family-Wise-Error-Whole-Brain-Corrected Voxel-Based Analyses (p<0.05) For Main Effects of Gender and of Condition in Women and Men

a. Main Effects of Gender							
Region	Volume (mm^3)	Volume (voxels)	Talairach X	Talairach Y	Talairach Z	Mean t-value	Std Value
Brodmann Areas 18, 19	36801	1363	4	-77	3	5.96	1.87
b. Main Effects of Condition in Women							
Region	Volume (mm^3)	Volume (voxels)	Talairach X	Talairach Y	Talairach Z	Mean t-value	Std Value
Anterior Cingulate, Putamen, Primary Auditory, Primary Sensory, Primary Motor, Insula, and Brodmann Areas 6, 8, 9, 10, 21, BA22, 40, 44, 45, 46, 47	225989	8370	8	6	7	4.88	1.82
Posterior Cingulate and R Brodmann Area 39	34292	1270	13	-53	30	5.32	2.18
L Brodmann Area 39	11366	421	-44	-60	28	4.47	1.15
c. Main Effects of Condition in Men							
Region	Volume (mm^3)	Volume (voxels)	Talairach X	Talairach Y	Talairach Z	Mean t-value	Std Value
Anterior Cingulate, Putamen, Thalamus, Primary Motor, Primary Sensory, Insula, Caudate, Hippocampus, Parahippocampus, and Brodmann Areas 6, 8, 9,10, 22, 37, 38, 39, 40, 44, 45, 46	445873	16514	2	-19	5	5.42	2.13

Table S2. Results of Family-Wise-Error-Whole-Brain-Corrected Voxel-Based Analyses (p<0.05) For Main Group and Group-by-Condition Interactive Effects

a. Main Effects of Diagnostic Group in Women							
Region	Volume (mm^3)	Volume (voxels)	Talairach X	Talairach Y	Talairach Z	Mean t-value	Std Value
Caudate, Brodmann Areas 10, 11, 21, and 47, and Insula	23942	887	9	14	3	6.098	1.98
b. Group-by-Condition Interaction in Women							
Region	Volume (mm^3)	Volume (voxels)	Talairach X	Talairach Y	Talairach Z	Mean t-value	Std Value
Cerebellum	14198	526	11	-60	-36	4.22	0.96
Caudate, Anterior Cingulate, and Brodmann Areas 47, 9 and 10	26169	969	-7	38	6	4.16	0.88
R Insula, Brodmann Area 40 and Primary Motor	13646	505	48	-13	21	3.88	0.59
Anterior Cingulate, Brodmann Areas 5, 6, 18, and 19, and Primary Sensory	50931	1886	-13	-22	41	4.27	1.09
c. Main Effects of Diagnostic Group in Men							
Region	Volume (mm^3)	Volume (voxels)	Talairach X	Talairach Y	Talairach Z	Mean t-value	Std Value
Anterior Cingulate, Putamen, Thalamus, Primary Motor, Primary Sensory, Insula, Caudate, Hippocampus, Parahippocampus, and Brodmann Areas 6, 8, 9, 10, 22, 37, 38, 39, 40, 44, 45, and 46	367950	13628	-1	-17	13	6.61	2.36
d. Group-by-Condition Interaction in Men							
Region	Volume (mm^3)	Volume (voxels)	Talairach X	Talairach Y	Talairach Z	Mean t-value	Std Value
Posterior Cingulate, Brodmann Areas 7 and 19	11938	442	5	-65	40	3.94	0.67

Table S3A. Results of Family-Wise-Error-Whole-Brain-Corrected Voxel-Based Analyses (p<0.05) For Group Differences in Women and Men For Each Condition

i. Group Differences During Stress Condition in Women							
Region	Volume (mm^3)	Volume (voxels)	Talairach X	Talairach Y	Talairach Z	Mean t-value	Std Value
Anterior Cingulate, Putamen, Insula, Amygdala, Hippocampus, Caudate, Thalamus, and Brodmann Areas 6, 8, 9, 10, 18, 19, 21 and 22	278107	10300	0	-10	10	2.55	0.47
Anterior Cingulate	10084	373	0	-3	37	2.5	0.33
Posterior Cingulate	2230	83	-10	-21	40	2.15	0.13
L ventromedial prefrontal cortex (Brodmann Area 11)	1389	51	-15	35	-14	2.2	0.17
R ventromedial prefrontal cortex (Brodmann Area 11)	1041	39	12	55	-9	2.23	0.17
L dorsomedial prefrontal cortex (medial Brodmann Area 9 and 10)	3276	121	-7	43	32	2.54	0.4
R dorsomedial prefrontal cortex (medial BA 9 and BA 10)	18146	672	12	45	22	2.53	0.42
L dorsolateral prefrontal cortex (lateral BA9 and BA10)	16652	617	-35	32	30	2.59	0.52
L Insula	8290	307	-37	-1	7	2.72	0.46
R Insula	13099	485	34	-1	6	2.82	0.5
L Inferior Frontal Gyrus (Brodmann Area 47)	2564	95	-27	24	-11	2.32	0.26
R Inferior Frontal Gyrus (Brodmann Area 47)	2428	90	25	23	-7	2.41	0.29
L Amygdala	260	10	-24	-2	-9	2.2	0.17
R Amygdala	327	12	21	-4	9	2.27	0.19
L Hippocampus	2637	98	-32	-19	-7	2.51	0.32
R Hippocampus	1320	49	28	-32	0	2.28	0.2
Ventral Striatum	20157	747	2	9	-1	2.77	0.48
ii. Group Differences During Drug Condition in Women							
Region	Volume (mm^3)	Volume (voxels)	Talairach X	Talairach Y	Talairach Z	Mean t-value	Std Value
Cerebellum	22943	850	-5	-63	-34	-2.43	0.35
R Anterior Cingulate, Posterior Cingulate, Primary Sensory, Primary Motor, Brodmann Areas 5, 7 and 39	20134	746	26	-36	40	-2.27	0.22
R Anterior Cingulate	3181	118	-1	-10	36	-2.22	0.17
Bilateral Posterior Cingulate	4862	180	-16	-43	29	-2.28	0.22
L Posterior Cingulate, Primary Sensory, Primary Motor, Brodmann Areas 5, 7 and 39	17877	662	-18	-50	34	-2.35	0.29
L Anterior Cingulate and Brodmann Area 6	13171	488	-19	-6	53	-2.38	0.37

iii. Group Differences During Neutral Condition in Women							
Region	Volume (mm^3)	Volume (voxels)	Talairach X	Talairach Y	Talairach Z	Mean t-value	Std Value
R Cerebellum	19257	713	31	-67	-30	2.46	0.43
Ventral Striatum, Anterior Cingulate, Brodmann Areas 6, 8, 9, 10, 45, 46 and 47	63096	2337	-10	31	14	2.42	0.36
L Inferior Frontal Gyrus (Brodmann Areas 45 and 46)	4602	170	-39	35	16	2.27	0.2
L Inferior Frontal Gyrus (Brodmann Area 47)	7071	262	-38	33	-3	2.38	0.26
R Inferior Frontal Gyrus (Brodmann Area 47)	522	19	26	22	-9	2.14	0.09
Anterior Cingulate	19720	730	3	34	6	2.48	0.36
Ventral Striatum	12278	456	-1	17	0	2.29	0.20
dorsolateral prefrontal cortex (Brodmann Areas 8, 9 and 10)	19078	707	-15	38	41	2.50	0.44
L Brodmann Areas 21, 22 and 37	10226	379	-56	-37	-10	2.56	3.39
iv. Group Differences During Stress Condition in Men							
Region	Volume (mm^3)	Volume (voxels)	Talairach X	Talairach Y	Talairach Z	Mean t-value	Std Value
Cerebellum	42186	1562	0	-57	-33	2.70	0.57
Anterior Cingulate, Putamen, Thalamus, Caudate and Brodmann Area 44	24823	919	-2	-3	9	2.36	0.32
Anterior Cingulate	1535	57	6	4	27	2.24	0.16
Ventral Striatum	10735	398	-9	2	5	2.43	0.36
Thalamus	7827	290	0	-12	7	2.35	0.31
Insula	820	30	-33	18	1	2.2	0.15
v. Group Differences During Drug Condition in Men							
Region	Volume (mm^3)	Volume (voxels)	Talairach X	Talairach Y	Talairach Z	Mean t-value	Std Value
Anterior Cingulate, Posterior Cingulate, Hippocampus, Caudate, Putamen, Thalamus, Insula, and Brodmann Areas 6, 7, 9, 10, 37, 38, 39, 40 and 47	433823	16068	-5	-17	12	2.61	0.51
Anterior Cingulate	15277	568	1	23	19	2.38	0.33
Posterior Cingulate	20837	772	-3	-23	31	2.7	0.49
Thalamus	22216	823	-2	-13	8	2.85	0.47
L Insula	7837	290	-38	11	3	2.88	0.63
R Insula	5547	205	34	16	4	2.77	0.5
L Caudate	4645	172	-13	3	11	2.89	0.5
R Caudate	4827	179	14	4	12	2.8	0.59
L Hippocampus	2128	79	-31	-30	-4	2.42	0.36

R Hippocampus	1636	61	31	-26	-8	2.46	0.39
L Putamen	7746	287	-27	0	4	3.05	0.52
R Putamen	7000	259	25	2	3	2.59	0.39
L dorsolateral prefrontal cortex	6933	257	-28	30	34	2.56	0.35
R dorsolateral prefrontal cortex	9855	365	36	30	31	2.61	0.50
L ventromedial prefrontal cortex	2113	78	-19	36	-10	2.52	0.38
R ventromedial prefrontal cortex	2558	95	14	34	-8	2.32	0.26
L Inferior Frontal Gyrus (Brodmann Area 47)	5883	218	-42	29	-6	2.66	0.45
R Inferior Frontal Gyrus (Brodmann Area 47)	3802	141	39	32	-6	2.40	0.29
vi. Group Differences During Neutral Condition in Men							
Region	Volume (mm^3)	Volume (voxels)	Talairach X	Talairach Y	Talairach Z	Mean t-value	Std Value
Anterior Cingulate, Posterior Cingulate, Primary Sensory, Primary Motor, Thalamus, Caudate, Putamen, Insula, Hippocampus, Amygdala, and Brodmann Areas 6, 8, 9, 10, 11, 19, 21, 22, 37 and 39	616035	22816	0	-17	11	2.61	0.48
Ventral Anterior Cingulate	10951	406	0	41	0	2.85	0.47
Dorsal Anterior Cingulate	8229	305	2	2	28	2.6	0.39
Posterior Cingulate	4890	181	1	-36	31	2.40	0.28
Thalamus	6217	230	-2	-19	6	2.36	0.28
L Hippocampus	2466	91	-32	-15	-11	2.76	0.41
R Hippocampus	4071	151	29	-19	-9	3.2	0.57
L Amygdala	1026	38	-23	-3	-12	2.51	0.32
R Amygdala	1215	45	25	-3	-12	3	0.46
L Insula	6829	253	-41	-4	4	2.66	0.41
R Insula	9489	351	38	1	4	2.62	0.36
L Ventral Striatum	8055	298	-24	0	0	2.69	0.39
R Ventral Striatum	10793	400	21	1	1	2.6	0.41
ventromedial prefrontal cortex (Brodmann Area 11)	5195	192	3	30	-11	2.55	0.40
Medial Frontal Cortex (medial Brodmann Areas 8, 9, 10)	25181	933	0	42	28	2.73	0.51
L Lateral Frontal Cortex (lateral Brodmann Area 10)	1926	71	-26	53	0	2.52	0.40
R Lateral Frontal Cortex (lateral Brodmann Area 10)	3948	146	22	54	6	2.41	0.30
L Inferior Frontal Gyrus (Brodmann Area 47)	3446	128	-41	22	-7	2.55	0.44
R Inferior Frontal Gyrus (Brodmann Area 47)	4160	154	35	26	-8	2.64	0.44

Table S3B. Results of Family-Wise-Error-Whole-Brain-Corrected Voxel-Based Correlations (p<0.05) For Drug-Cue-Induced Craving and Stress-Cue-Induced Craving in Women and Men

i. Correlations of Drug-Cue-Induced Craving in Women							
Region	Volume (mm^3)	Volume (voxels)	Talairach X	Talairach Y	Talairach Z	Mean r Value	Std Value
Cerebellum, Brainstem, Thalamus and Caudate	75441	2794	1	-49	-25	-0.59	1.98
R Hippocampus, Parahippocampus and Brodmann Area 38	12310	456	37	-2	-22	-0.47	0.19
L Hippocampus, Parahippocampus, and Brodmann Areas 20, 21, 37 and 38	22742	842	-47	-16	-11	-0.48	0.20
ii. Correlations of Drug-Cue-Induced Craving in Men							
Region	Volume (mm^3)	Volume (voxels)	Talairach X	Talairach Y	Talairach Z	Mean r Value	Std Value
L Cerebellum and Brodmann Areas 19, 20, 37 and 39	75441	2794	1	-49	-25	-0.59	1.98
Thalamus, Posterior Cingulate, Hippocampus, and Brodmann Areas 6, 30, 40 and 44	12310	456	37	-2	-22	-0.47	0.19
iii. Correlations of Stress-Cue-Induced Craving in Men							
Region	Volume (mm^3)	Volume (voxels)	Talairach X	Talairach Y	Talairach Z	Mean r Value	Std Value
L Visual Cortex (Brodmann Areas 18, 19 and 37)	17207	637	-28	-73	-2	0.19	0.27
R Visual Cortex (Brodmann Areas 18, 19 and 37)	11011	407	22	-67	-8	0.20	0.17